The locomotor kinematics and ground reaction forces of walking giraffes

Christopher Basu[1*], Alan M. Wilson[1], John R. Hutchinson[1]

[1] Structure & Motion Laboratory, Royal Veterinary College, Hawkshead Lane, North Mymms, Hatfield, Hertfordshire AL9 7TA

* Corresponding author's email address: christopherbasu@gmail.com

SUMMARY STATEMENT

Giraffes' specialised anatomy confers a feeding advantage; how does this affect locomotion? We measured the forces and motions of walking giraffes - their gait was surprisingly similar to other mammalian quadrupeds.

ABSTRACT

Giraffes (*Giraffa camelopardalis* Linnaeus 1758) possess specialised anatomy. Their disproportionately elongate limbs and neck confer recognised feeding advantages, but little is known about how their morphology affects locomotor function. In this study, we examined the stride parameters and ground reaction forces from three adult giraffes in a zoological park, across a range of walking speeds. The patterns of GRFs during walking indicate that giraffes, similar to other mammalian quadrupeds, maintain a forelimb-biased weight distribution. The angular excursion of the neck has functional links with locomotor dynamics in giraffes, and was exaggerated at faster speeds. The horizontal accelerations of the neck and trunk were out of phase, compared with the vertical accelerations which were intermediate between in and out of phase. Despite possessing specialised morphology, giraffes' stride parameters were broadly predicted from dynamic similarity, facilitating the use of other quadrupedal locomotion models to generate testable hypotheses in giraffes.

KEYWORDS: Locomotion, Giraffe, Quadruped, Ground reaction force, Kinematics, Cursorial

LIST OF SYMBOLS AND ABBREVIATIONS

a1, a2, a3	Fourier coefficients
ANCOVA	Analysis of covariance

ANOVA	Analysis of variance
BM	Body mass (kg)
BW	Body weight (N)
COM	Centre of mass
FL	Forelimb
Fr	Froude number
F_Z	Vertical force (N)
g	Acceleration due to gravity (ms^{-2})
GRF	Ground reaction force (N)
h	Shoulder height (m)
HL	Hindlimb
OLS	Ordinary least squares
m	mass (kg)
PPE	Percentage prediction error (%)
ROM	Range of motion
RMSE	Root mean square error
SD	Standard deviation
T_{STANCE}	Stance duration (s)
u	speed (ms^{-1})
ω	angular frequency (rad s^{-1})

INTRODUCTION

Giraffes (*Giraffa camelopardalis* Linnaeus 1758) represent an extreme of many biological variables. They are the tallest living animal, and the heaviest ruminant mammal. Whilst their extreme height confers a documented feeding advantage (Cameron and du Toit, 2007), the combination of disproportionately long neck and limb length with large body mass is also of consequence to other

common behaviours, such as locomotion. For example, do giraffes' disproportionately long legs permit them to use relatively long stride lengths at a given speed? Does the mass of the head and neck cranially displace the centre of mass (COM) when compared with other cursorial quadrupeds? Beyond the influential work of Dagg (Dagg and Vos, 1968a; Dagg, 1962; Dagg and Vos, 1968b) and Alexander (Alexander et al., 1977), giraffe gait dynamics remain seldom studied. In particular, there is no comprehensive examination of giraffe ground reaction forces (but see Warner et al., 2013, which included a giraffe GRF as part of an interspecific comparative dataset).

The focus of this study was (1) to quantify the basic kinematics and ground reaction forces (GRFs) of the giraffe walking gait, (2) to question whether these parameters diverge from the trends predicted from other mammalian quadrupeds, (3) to quantify the angular kinematics of the neck, and (4) to assess whether these parameters are speed dependent. In this study, we analyse such data from giraffes as they walk through an experimental setup in a zoological park

Walking is giraffes' dominant locomotor behaviour, as the majority of their daily routine is spent foraging (Innis, 1958). The terminology used to describe the walking gait varies. Giraffes' walk has been referred to as a pace, a walking pace, a rack, and an ambling walk (Bennett, 2001; Dagg, 1962; Innis, 1958; Kar et al., 2003). The use of differing terminology implies that giraffes' walking gait is specialised when compared with other mammalian quadrupeds, but this has not been tested.

A useful method for examining symmetrical gaits, where footfalls of the left and right side of the body are evenly spaced through time, is to quantify duty factor (the proportion of the stride that a foot contacts the ground, Eqn 1) and limb phase (the fraction of the stride between the forelimb (FL) footfall, relative to the ipsilateral hindlimb (HL) footfall, Eqn 2). Using these two dimensionless numbers, symmetrical gaits may be compared at the level of the individual or species (Hildebrand, 1976).

$$duty\ factor = \frac{stance\ duration}{stride\ duration} \quad \text{Eqn 1}$$

$$limb\ phase = \frac{Time_{FL\ foot\text{-}on\ event} - Time_{HL\ foot\text{-}on\ event}}{stride\ duration} \quad \text{Eqn 2}$$

Giraffes use lower stride frequencies (and consequently longer stride lengths) at running speeds compared with other African ungulates (Alexander et al., 1977), a strategy which may be facilitated by their elongate limbs. It is unclear whether a similar strategy is employed at walking speeds. An expansion of this point is to question whether the unusual morphology of giraffes might have shifted their locomotor dynamics away from the general patterns predicted for walking quadrupedal

mammals. The dynamic similarity hypothesis provides a useful framework for addressing this question. The principle of this theory assumes that subjects are geometrically similar to each other (Alexander and Jayes, 1983). In their study, Alexander and Jayes demonstrated that the broad trend in body shape *versus* mass is isometric (Table 1 of the paper), although noted that giraffes may be an 'extreme example' of how some quadrupedal mammals are not geometrically similar (e.g. they state that giraffes 'have twice the shoulder height of rhinoceros of equal mass'). In light of this, it remains uncertain whether giraffes' geometric dissimilarity is also associated with dynamic dissimilarity – in which case locomotor dynamics should diverge from other quadrupeds.

Stride parameters often vary as a function of speed. Stride duration, stance duration and duty factor typically vary inversely with speed, as demonstrated by a wide range of terrestrial animals (Hutchinson et al., 2006, Walker et al., 2010, Pfau et al., 2011, Shine et al., 2015, Gatesy and Biewener, 1991), including a study of an adult giraffe (Dagg, 1962). Studying how giraffes' stride and force parameters change with speed gives mechanistic insight as to how different speeds are attained, and whether giraffes' derived anatomy facilitates higher walking speed. Lameness is a welfare issue for giraffes in zoological collections (Hummel, 2006), so an understanding of giraffe gait at varying speed is one step closer to quantifying gait pathology.

The distribution of vertical impulse (the integral of vertical force throughout the stride duration) is unequal in most quadrupeds studied, with the forelimbs bearing a larger proportion of body weight than the hindlimbs (Alexander et al., 1979; Griffin et al., 2004; Hudson et al., 2012; Lee et al., 1999; Shine et al., 2015; Witte et al., 2004) . This contrasts with most primates, which maintain a hindquarter biased weight distribution (Raichlen et al., 2009). One explanation for a forequarter biased distribution is that it is related to the mass of the head and neck. Indeed, disproportionate increases of these masses may lead to a cranial shift of the centre of mass relative to foot position (Bates et al., 2016).

The role of the head and neck in quadrupedal locomotion is less frequently studied. In an adult giraffe, the mass of the head and neck accounts for approximately 10% of body mass (Mitchell et al., 2013; Simmons and Scheepers, 1996). This is similar to the proportion seen in the horse (Buchner et al., 1997), but in giraffes this mass is distributed over a longer distance, and the neck is carried with a more vertical posture (Dagg, 1962; Loscher et al., 2016).

In one comparative study of ungulate neck motion (Loscher et al., 2016), the majority of walking ungulates exhibited cyclical vertical neck acceleration which was out of phase with vertical trunk acceleration. This phase relationship likely results in net kinetic energy savings, and potential metabolic savings. In giraffes, the vertical phase relationship was notably modest in comparison with

other ungulates, implying that mechanical energy conservation in the vertical plane is similarly modest. The horizontal phase relationship between neck and trunk acceleration was not studied, so it is as yet unclear whether neck motion in the horizontal plane contributes to or reduces COM acceleration.

Our aims for this study are: first, to identify the footfall patterns used by giraffes during walking; second, to quantify the stride parameters and ground reaction forces of giraffes' walking gait and assess how these change with speed; third, to measure the angular kinematics of the neck across multiple strides; and finally, to assess to what degree giraffes conform to the predictions of dynamic similarity (and if applicable, in what ways they do not).

We specifically question whether or not giraffes use a true pacing gait, where a pace is defined with a limb phase < 6.25% (Pfau et al., 2011); whether giraffes increase stride length over frequency to achieve faster walking speeds; how neck excursion relates to gait parameters; and we quantify the percentage prediction error (PPE) associated with the predictions of dynamic similarity for giraffes.

METHODS

Animals

We collected synchronised video and force plate data from three adult Reticulated giraffes (Table 1) kept at a zoological institution (Whipsnade Zoo, Bedfordshire, United Kingdom). The use of skin markers was not possible, as the animals were not accustomed to this type of manual handling. The giraffes were deemed as fit to participate by zoo veterinary staff. Giraffe 3 had a history of overgrown hoofs on both forefeet, but no sign of lameness was detected by veterinary staff throughout the course of the study, and the data were screened for potential subject effects (see Statistical Analysis). This work was conducted with ethical approval from the Royal Veterinary College, University of London; Clinical Research Ethical Review Board number URN 2016 1538.

Data collection

We mounted a 6.0 x 0.9 m array of ten AMTI three-axis force plates (Advanced Mechanical Technology, Watertown, Massachusetts USA) with Hall-effect sensors onto a custom-built steel rack, into the giraffes' sand covered outdoor enclosure. The rack was buried 5 cm below the substrate surface, and covered with sand; this was necessary to allow the giraffes to display normal locomotor behaviour, and to prevent inadvertent excavation around the edges of the rack. The array was positioned along a fence, with enough room at either end for giraffes to accelerate or decelerate prior to walking over the force plates (Fig. 1).

The animal keepers led the giraffes back and forth across the force plate array, motivating the animals by carrying foodstuffs ahead of them. Data were collected over the course of one hour per day, for six days spread across two batches of data collection, separated by a period of three months. The keepers elicited a range of giraffe speeds by varying their own speed.

The force plates' voltage output was recorded using an analogue-to-digital data acquisition instrument (National Instruments, Newbury, Berkshire UK) connected to a laptop. A manual trigger was used to start 30 second recordings of the force plate signals, at 240 Hz per channel. Data acquisition was controlled using a custom-written LabView (National Instruments, Newbury, Berkshire UK) script.

Two Hero3+ cameras (GoPro, San Mateo, California USA) were mounted perpendicular to the fence. Camera 1 was aimed at the centre of force plates 1-5, and camera 2 was aimed at force plates 6-10. Video data were collected at a frame rate of 120 Hz. The force plate trigger was also connected to an LED light, positioned to be in the field of view of both cameras, so that the start of the 30 second recordings could be synchronised to video. The study area was calibrated at the start of each day of data collection; a grid of known dimensions was walked through the space, allowing pixel distances in the digital videos to be converted to metres. Cameras subsequently were not moved. A repeat calibration to assess for inadvertent (e.g. wind induced) movement was not performed after each data collection, as it was not possible to access the giraffe paddock once the giraffes were outdoors.

Data processing

The force plate signals were processed with custom Matlab (Mathworks, Natick, Massachusetts USA) software, which took raw voltages and converted to calibrated ground reaction forces, using plate-specific calibration matrices. Calibrated forces were filtered using a zero-phase (back and forth) 4^{th} order Butterworth filter with a 6Hz cut-off. A further custom script calculated peak forces and impulses.

The camera distortion was corrected using GoPro Studio 2.5 (GoPro, San Mateo, California USA). The cameras were calibrated using the grid of known dimensions as a reference, allowing each pixel in the field of view to be assigned a calibrated displacement from the image origin. The video data were digitized using DLTDV6 (Hedrick, 2008). To measure speed, neck angle and stride parameters, we devised a virtual marker system consisting of the coronary band of each foot, a point behind the ear, a point on the giraffes' withers, and a point at the lumbosacral region (Fig. 2A). Each giraffe had a comparable virtual marker system which was adhered to throughout data processing.

Strides were defined as stance phase followed by swing phase. Stride parameters were measured from the near-side of the body with respect to the cameras during each trial. Foot contact times were determined using a consistent combination of force plate and video data. Stance duration, indicated by foot-on and foot-off events, was determined using the force/time derivative from force plate data, where a threshold of 1 N per millisecond was used to determine the timing of rapid loading and unloading associated with the stance phase. The subsequent foot-on event (indicating the end of the stride) was frequently not available from force plate data, because the giraffes commonly placed contralateral forelimbs and hindlimbs onto the same force plate, resulting in mixed GRF recordings. Instead we used the digitised foot motion and a velocity threshold of 1 ms^{-1} to denote the end of the stride (Starke and Clayton, 2015). Stride length was calculated as the displacement of the foot between the start and end of the stride, and stance distance was defined as the displacement of the withers during the stance duration.

Speed was determined for each stride by calculating the mean velocity of the withers and lumbosacral points over the duration of the stride. Two digitised points were used to reduce the possibility of positional error. Speeds were converted to Froude number (Eqn 3), where u = speed (ms^{-1}), g = acceleration due to gravity (9.81 ms^{-2}) and h = shoulder height (m), to allow comparisons between giraffes and other species (Alexander and Jayes, 1983).

$$Fr = \frac{u^2}{gh} \qquad \text{Eqn 3}$$

We only included strides that featured steady-state locomotion. We measured the velocity of the withers and lumbosacral digital markers over 0.2 seconds during the start and end of the stride, and compared any difference with the overall speed. Strides with acceleration or deceleration over 20% of the overall speed were excluded from the analysis (Shine et al., 2015). The remaining strides were checked again for changes in speed, by calculating the goodness of fit of an ordinary least squares (OLS) linear model to the time series data for the withers marker. Any strides with R^2 values < 97.5% were excluded from the analysis.

Body weight (BW; in Newtons) was determined for each giraffe by calculating the time-averaged vertical impulse of an entire stride cycle, where all four feet made complete contact with the force plate array. Five measurements of BW per giraffe were used to calculate the mean values, which were subsequently used to standardise selected force parameters. Vertical, craniocaudal and mediolateral GRFs were included in the analysis. Peak forces were standardised by body weight. In steady-state locomotion, the sum of the vertical impulses from all four feet can be defined as:

$$\sum \text{Impulse}_{\text{VERT}} = \text{BW} * \text{stride duration} \qquad \text{Eqn 4}$$

This can be rearranged to:

$$\frac{\sum \text{Impulse}_{\text{VERT}}}{\text{BW} * \text{stride duration}} = 1 \qquad \text{Eqn 5}$$

We therefore further standardised $\text{Impulse}_{\text{VERT}}$ to body weight and stride duration. Craniocaudal impulses ($\text{Impulse}_{\text{CC}}$) were also standardised in the same manner. The GRFs recorded in the current study were from independent strides, as we did not obtain ipsilateral fore- and hindlimb footfalls from the same stride. We estimated the relative contribution of fore- and hindlimbs to COM balance, by separately modelling $\text{Impulse}_{\text{VERT}}$ for the fore- and hindlimbs using OLS linear regression. By looking at the $\text{Impulse}_{\text{VERT}}$ predictions at a given speed, the relative distribution of body weight between the forelimbs and hindlimbs could be quantified.

Fourier analysis

GRF components have previously been modelled using a Fourier analysis (Alexander and Jayes, 1980; Hubel and Usherwood, 2015), where the GRF_{VERT} profile was represented by three sine wave coefficients of the form:

$$\frac{F_Z}{mg} = a_1 \sin\left(\pi \frac{t}{T_{stance}}\right) + a_2 \sin\left(2\pi \frac{t}{T_{stance}}\right) + a_3 \sin\left(3\pi \frac{t}{T_{stance}}\right) \qquad \text{Eqn 6}$$

The three coefficients provide a means to quantitatively describe the shape of the force profile over the stance duration, and allow quantitative comparison with other GRF data. In Eqn 6, the coefficients dictate the magnitudes of different shaped sine waves during the stance duration (T_{stance}); $a1$ dictates the magnitude of a single-peaked positive sine wave, a_2 a positive followed by negative wave, and a_3 a doubled-peaked positive wave.

A Fourier series was fitted to representative GRF_{VERT} data from the forelimb and hindlimb, by finding the solution that minimised the root mean square error (RMSE) between the experimental and fitted data in custom Matlab code. We used Fourier constants to model how the GRF_{VERT} profile changed as a function of speed. The angular neck kinematics of the giraffe were also fitted to a Fourier series, to allow for future comparisons with other quadrupedal species.

Statistical modelling

Statistical procedures were carried out using the Matlab Statistical Toolbox. Variables were first assessed for normality using a Kolmogorov-Smirnov test. Any differences in the kinematic and kinetic parameters with regard to the forelimb versus the hindlimb were first identified using an analysis of co-variance analysis (ANCOVA), with stride and force parameters as the dependant

variable, speed as the covariate, and fore or hindlimb as the independent variable. Differences between fore and hindlimb data in terms of regression slope and parameter mean (adjusted to compensate for speed variation) were tested as part of the ANCOVA. Data for the forelimb and hindlimb were subsequently treated separately if a significant difference was identified. To assess the significance of regression slopes, OLS linear regressions were subsequently performed using speed as the independent variable, and stride and force parameters as the dependant variable. To correct for the increase in Type 1 error rate associated with multiple statistical comparisons, we used the Benjamini – Hochberg procedure (Benjamini and Hochberg, 1995). This procedure reduces the probability of Type I error by cumulatively adjusting the critical values for null hypothesis rejection, up to a false discovery rate. We applied this correction to the ANCOVA and OLS regression comparisons, using a false discovery rate of 0.05.

The potential for inter-giraffe subject effects on stride and force parameters was separately assessed using mixed effect linear modelling. Stride length and peak force were each modelled as response variables, with speed as the predictor and giraffe identity as an additional fixed effect. The significance of giraffe identity in both stride length and peak force was tested by comparing models with and without the effect, using a likelihood ratio test.

RESULTS

Seventy-five strides featuring a complete ground reaction force and associated kinematics were analysed; representing approximately 5% of the total dataset. The remaining strides were excluded on the grounds of having excessive acceleration or deceleration, obscured footfalls or incomplete ground reaction forces.

Since paired forelimb and hindlimb ground reaction forces from the same stride could rarely be recorded, the GRF data used in the analysis are from isolated fore- or hind- footfalls (Table 1). Parameter means and/or regression slopes were different between the forelimbs and hindlimbs (Table S1), aside from stride length, stride frequency and peak propulsive force. All parameters followed a normal distribution, and giraffe identity did not have a significant effect on stride length or peak force (likelihood ratio test, $p = 0.84$ and $p = 0.97$ respectively).

Kinematics

Despite keepers' attempts to evoke a wide range of speeds, the giraffes elected to use a narrow speed range from 0.74 to 1.3 ms^{-1}; with a mean speed of 0.98 ms^{-1} (0.054 Fr), a combined mean duty factor of 0.70 and mean limb phase of 0.14. In conventional gait terminology (Hildebrand, 1989), this can be expressed as a 70:14 symmetrical gait, or a lateral sequence walk (Fig. 3).

All linear regressions are summarised in Table S2. Faster speeds were associated with marked increases in stride length (Fig. 4A), and subtle increases in stride frequency (the inverse of stride duration); for every 1 ms^{-1} increase in speed, stride length and frequency increased by a factor of 1.3 and 0.17 respectively. Stance duration decreased whilst swing duration was maintained across the speed range, accounting for the observed drop in duty factor and stride duration (Fig. 4B and 4C) with faster speeds. Mean duty factors were 1.07x greater in the forelimb compared with the hindlimb ($p < 0.001$, Table S1).

The neck oscillated twice during any given stride (Fig. 2C); peak dorsal extension occurred during each (left and right) early forelimb stance, with peak ventral flexion occurring in each forelimb mid-stance. The time series of neck angle for each trial was modelled using a two term Fourier series with mean RMSE of 0.074° (Table S3). The range of motion (ROM) of the neck during stance had a positive relationship with speed ($p = 0.015$), indicating that the amplitude of neck ROM was greater at faster speeds (Fig. 2B).

Ground reaction forces

Forelimb and hindlimb GRF_{VERT} profiles were comparable with the 'M' shaped profiles seen in other walking animals, but had some contrasting features (Fig. 5). In the forelimb, two GRF_{VERT} profile shapes were observed. Giraffes 1 and 3 displayed shape 'F1', typified by a reduced early-stance peak; whilst Giraffe 2 displayed type 'F2', consisting of two pronounced peaks (Fig. 5C and 5D). In each of the shapes, the late stance peak was typically higher than in early stance. Both profiles were observed at similar speeds (mean of 0.05 and 0.06 Fr respectively), so we do not attribute this variation in GRF_{VERT} to be a function of walking speed. Two distinct hindlimb GRF_{VERT} profile shapes were also apparent (Fig. 5E and 5F), but this variation occurred both within and between individuals. Shape H1 had two peaks, whereas shape H2 had an additional third peak, occurring during mid-stance.

To quantitatively describe the shape of the GRF_{VERT} profiles, representative data were fitted to a Fourier series. The resulting fits have low RMSEs (mean = 0.06, Table S4), and the profiles are comparable with a Fourier analysis of human GRF_{VERT} profiles (Hubel and Usherwood, 2015). The shape of the forelimb GRF_{VERT} profiles, as modelled by Fourier coefficients, changed as a function of

speed, with each coefficient increasing in magnitude (Fig. 6A). In contrast, there was no apparent relationship between hindlimb GRF_{VERT} profile and speed (Fig. 6B).

Fourier modelling did not distinguish between the two observed hindlimb GRF_{VERT} shapes. Adding extra Fourier terms up to the next odd harmonic further reduced the RMSE in both H1 and H2, but this did not discriminate between these shapes. Instead, the presence of a third (mid-stance) peak was established by qualitatively grouping the hindlimb GRF_{VERT} profiles according to the presence or absence of a third peak, and testing (using a one-way ANOVA) whether this grouping had an effect on the difference between peak force at mid-stance and the overall peak force. The presence of a third peak was statistically distinguishable from background variation (ANOVA $p = 0.003$).

Peak vertical forces did not change significantly within the measured speed range (Fig. 7A), but were 1.9 times greater in the forelimbs. When standardised by BW and stride duration (Fig. 7B), forelimb and hindlimb $Impulse_{VERT}$ did not change significantly with speed ($p = 0.269$ and $p = 0.047$ respectively). The sum of standardised forelimb and hindlimb $Impulse_{VERT}$ should account for 50% of BW (the other half being accounted from contralateral limbs). The mean values here summed to 48% of BW, with a FL:HL vertical force ratio of 65:35. The unaccounted 2% is attributed to measurement and statistical error; particularly because forelimb and hindlimb data were from separate strides. The measurement error can be demonstrated by the standard deviation of the repeated body mass measurements for each individual, which ranged from 1.3% – 1.6% of BW, whilst the statistical error was demonstrated by the RMSE seen in the forelimb and hindlimb linear models, which was 2% in both cases.

Craniocaudal ground reaction forces (GRF_{CC}) in the fore and hindlimbs were characterised by negative (braking) forces in early stance, changing to positive (propulsive) forces in late stance (Fig. 5A and 5B). Peak braking force in the forelimb increased in magnitude with speed ($p = 0.003$). The ANCOVA adjusted mean net $Impulse_{CC}$ (standardised to BW and stride duration) were higher in the HL versus FL (0.006 and -0.002 respectively, ANCOVA $p = 0.012$, Table S1). Net $Impulse_{CC}$ was statistically indistinguishable from zero in the forelimb (t-test $p = 0.2614$), whilst being positive in the hindlimb (t-test $p = 0.003$). The ANCOVA adjusted mean positive $Impulse_{CC}$ were equal in the FL and HL ($p = 0.584$). In contrast, the ANCOVA adjusted mean negative $Impulse_{CC}$ were of greater magnitude in the FL ($p<0.001$, Table S1). Mediolateral forces were of low magnitude, accounting for 0.7% of total impulse.

DISCUSSION

The giraffes in the current study used a lateral sequence walk, or in Hildebrand terms, a 70:14 gait (Fig. 3). This is a typical walking gait used by quadrupeds, and is different from a pacing gait, which can be seen in some running horses, dogs and camels (where limb phase is below 6.25%). Despite popular accounts that giraffes pace, at no point in this study did the limb phase reach a level consistent with this definition; similar to the confusion surrounding which footfall pattern alpacas use (Pfau et al., 2011).

The giraffes were able to achieve faster walking speeds whilst maintaining relatively conserved stride frequencies, illustrating that giraffes increase walking speed predominantly by taking longer strides. It is possible that the narrow range of observed stride frequencies in giraffes are close to their limbs' natural frequency. Assuming a pendulum model of walking, increases of stride frequency in excess of natural frequency are met with a sharp increase in force and work requirements. In humans, such increases are associated with corresponding increases in metabolic cost (Doke et al., 2005). Larger organisms such as giraffes may be particularly sensitive to this relationship, given their relatively large limb inertia. Giraffes may preferentially select stride frequencies which are optimised for metabolic economy (Loscher et al., 2016).

Duty factors were consistently greater in the forelimb compared with the hindlimb (Fig. 4C). The greater forelimb duty factors observed here offset the higher peak force experienced in the forelimb by spreading the impulse over a longer stance duration. If duty factors remain greater in the forelimb at near-maximal speed, they may have a role to play in maintaining tissue safety factors (Biewener, 1983).

Duty factor is causally related to peak force (Alexander et al., 1979; Witte et al., 2004). Each foot must support a proportion of the total body weight over the course of a stride. Since duty factor was lower at faster speeds, $Impulse_{VERT}$ was therefore compressed into shorter stance durations; as a result we expected to see an increase in peak vertical force with speed. Yet, there was no significant change with speed (Fig. 7A). We have considered the presence of substrate as an unlikely explanation for this result. Compliant substrates are associated with dampening of the initial impact GRF, not peak mid-stance vertical force, when compared with firm substrate (Parkes and Witte, 2015). This relationship may explain the lack of an impact peak in the observed GRFs. Deep wet sand substrates are also associated with a reduction of peak mid-stance force, but this is associated with the lengthening of stance duration (Crevier-Denoix et al., 2010). We speculate that peak forces in giraffes are instead dampened by compliant musculotendon units. Giraffe tendons are long, and relatively slender (e.g. the digital flexor muscles), and it is reasonable to hypothesise that they have a high amount of compliance (Zajac, 1989). Since compliant limbs are observed to dampen peak

force (McMahon et al., 1987; Ren et al., 2010), giraffes may conserve peak force at a consistent level across slow walking speeds.

The measurement of vertical impulses from independent forelimb and hindlimb strides (Fig. 7B) suggests that giraffes maintain a FL:HL vertical impulse distribution of 65:35 across a modest walking speed range. By this measure, giraffes are broadly similar to most other quadrupedal mammals, despite having a large (and long) mass of neck and head attached to the cranial thorax.

$Impulse_{CC}$ values are often different in quadrupeds' fore- and hindlimbs; owing to those limbs' specialised functions in braking and propulsion (Griffin et al., 2004; Pandy et al., 1988). Our results indicate that propulsion in giraffes is shared between the forelimb and hindlimb. In contrast, braking impulses were significantly greater ($p < 0.001$, Table S1) in the forelimb, indicating that the giraffe forelimb has a dominant role in decelerating the COM during steady-state locomotion, a feature which is shared by many other non-primate quadrupeds; including dogs, goats, elephants and grizzly bears (Griffin et al., 2004; Pandy et al., 1988; Ren et al., 2010; Shine et al., 2015).

Giraffe neck oscillation during walking is tied with stride frequency, whereby the neck oscillates twice throughout one walking stride period. We assessed the biomechanical importance of this oscillation by estimating the periodic tangential acceleration of the neck and its phase relative to the acceleration of the trunk. For this purpose, we modelled the neck and head as a massless hinged rod with a point mass of 80kg at the distal end. The rod's length (r) was equal to the radius of gyration of the neck-head system, assuming the simplified geometry of a uniform cylinder and an overall length of 1.5 m (Eqn 7). Kinematic data were then used as inputs to derive the tangential acceleration of the neck. In this model, the point mass oscillates around a starting angle (θ, measured from a vertical reference) with magnitude (q_0) and angular frequency (ω). q_0 was neck ROM/2 (measured from a vertical reference), and ω (rad s^{-1}) was dependent on the stride duration (Eqn 8). The sine oscillation was offset by *a* seconds, to match the phase of the oscillation observed in experimental data. *a* was derived by fitting the neck angle in each trial to Eqn 9, using the 'fit' function in Matlab. ROM and ω were derived from the mean values from 46 trials (Table S5).

$$r = \frac{neck\ length}{\sqrt{3}} \quad \text{Eqn 7}$$

$$\omega = \frac{2\pi}{0.5 * stride\ duration} \quad \text{Eqn 8}$$

Neck angle (q) at each time step (t) may then be modelled as follows:

$$q = q_0 * \sin(\omega(t + a)) + \theta \quad \text{Eqn 9}$$

The goodness of fit of this model was checked for each trial, with a resulting mean RMSE of 2.3° and SD of 1.5°. The horizontal and vertical displacement of the neck (Fig. S1) at each time step was then expressed as:

$$horizontal\ displacement = r * \sin(q) \quad \text{Eqn 10}$$

$$vertical\ displacement = r * \cos(q) \quad \text{Eqn 11}$$

Eqns 10 and 11 were differentiated twice with respect to time, to derive the neck's acceleration at each time step. Peak neck accelerations were multiplied by neck mass to calculate horizontal and vertical tangential force. This model predicts that giraffes' peak vertical neck accelerations are low, with the resulting force equalling 1.2% of BW. Predicted peak horizontal accelerations are also modest, with a force of 0.8% BW (accounting for approximately 15% of peak GRF_{CC}). At faster speeds, we predict that neck tangential forces are greater, as the model predicts an increase to the square of stride frequency, and we independently observed an increase in neck ROM with walking speed (Fig. 2B).

The effect of the neck's tangential forces on the COM is dependent on the phase relationship between the neck and the trunk. We used the modelled neck accelerations and mean GRFs to calculate the phase relationship between the accelerations of the trunk and neck. Vertical and horizontal accelerations were evaluated separately. We assumed that the relationship between neck force ($Force_{NECK}$), trunk force ($Force_{TRUNK}$) and COM of mass force ($Force_{COM}$) was as follows:

$$Force_{TRUNK} = Force_{COM} - Force_{NECK} \quad \text{Eqn 12}$$

COM forces can be determined by summing all ground reaction forces (GRFs) throughout the stride cycle. In this instance, a COM force time series was modelled by superimposing mean forelimb (FL) and hindlimb (HL) GRFs, temporally spaced using mean limb phase and duty factor. GRFs were summed to derive an estimation of $Force_{COM}$. COM acceleration (Acc_{COM}) was calculated as:

$$Acc_{COM} = \frac{Force_{COM}}{body\ mass} \quad \text{Eqn 13}$$

The neck's acceleration (Acc_{NECK}) in the horizontal and vertical planes were calculated by double differentiating the displacement of the neck's point mass (Fig. S1) with respect to time.

$Force_{NECK}$ was derived as follows:

$$Force_{NECK} = Acc_{NECK} \times 0.1BM \quad \text{Eqn 14}$$

$Force_{TRUNK}$ was derived from Eqn 12, and its acceleration (Acc_{TRUNK}) calculated assuming that its mass

(also encompassing the limbs) was 0.9 x body mass. The acceleration due to gravity (9.81 ms^{-2}) was subtracted from the vertical components of acceleration.

The phase relationship between neck and trunk acceleration was calculated as the fraction of the stride between their time series' maxima or minima. A phase of 0% (i.e. in phase oscillation) between neck and trunk acceleration would indicate that the COM (the sum of neck and trunk) experiences greater acceleration and velocity - and therefore greater kinetic energy - than just the trunk alone. In this situation, the neck is a potential a burden for the giraffe's walking gait. On the other hand, a phase of 25% of the stride (i.e. out of phase oscillation) would indicate that COM acceleration and velocity is instead diminished by neck movement; this would indicate a mechanical energy saving mechanism.

We found that horizontal neck acceleration in giraffes is largely out of phase with the trunk, with a phase relationship of 23% (Fig. 8A). For example, as the trunk is decelerated during the beginning of stance, the mass of the neck accelerates in the opposite direction. In a global inertial frame the neck therefore experiences little horizontal acceleration. This is likely to be a result of the neck's inertia and its degrees of freedom with the trunk. In effect the horizontal motion of the neck is passively decoupled from the rest of the body. As a consequence, we expect that horizontal COM forces (measured as GRF_{CC}) are attenuated by neck motion. This may explain why we did not observe any trends between GRF_{CC} and walking speed.

A parallel may be drawn between the horizontal phase relationship of the giraffe and the modern 'Martini Glass' riding style in horse racing. In this riding style, the jockey oscillates their body in the horizontal plane, out of phase with the horizontal oscillations of the horse's trunk, effectively decoupling themselves from the trunk's horizontal accelerations. The advantage of this riding style is that the horse does not have to accelerate or decelerate the rider in the horizontal plane, which may be otherwise detrimental to the horse's athletic performance (Pfau et al., 2009). We propose that giraffes may benefit from a similar mechanism, albeit at walking speeds.

The phase relationship between the vertical oscillations of the neck and trunk was 15% (Fig. 8B), similar to previous findings in giraffes (Loscher et al., 2016). This suggests that mechanical energy conservation is modest with respect to supporting the weight of the head and neck. As accelerations are predicted to increase with the square of stride frequency, the amount of limb work required to support the bodyweight may place a constraint upon maximum walking speed. Given the increase in metabolic energy associated with swinging appendages beyond their natural frequency (Doke et al., 2005), neck inertia may be one factor which influences gait transition.

One limitation of the above modelling was the variable agreement between Eqn 9 and experimentally measured neck angles. A potential source of error was our method of motivating the giraffes using feedstuffs, which may have introduced artefactual variation in neck kinematics. We therefore reality-checked the modelled neck-trunk phase calculations against kinematic data. The phase relationship between the virtual withers and neck markers was calculated from each experimental trial (n=46). The mean horizontal phase from these trials (Fig. 8C) was 22% (± SD of 4.7%) and the mean vertical phase (Fig. 8D) was 17% (± SD of 4.0%); thus there was good agreement between the modelled and empirical data.

The influence of neck posture and gravity on the mechanical cost of swinging the neck adds an additional layer of complexity to this system, as does the involvement of the nuchal ligament, which likely passively stores and releases elastic energy. A muscle-driven forward dynamics simulation would be a novel method of simulating the effect of stride frequency and neck posture on limb work.

Our signal-to-noise ratio has been affected by the low range of speeds observed, and the scatter induced by our experimental setup. During data collection, the giraffe keepers made efforts to encourage a wider range of speeds, but this resulted in poor subject compliance and (at best) excluded trial data. The observed speed range may therefore be viewed as being semi-selected by the giraffes. Our choice to use a sandy substrate on top of our force platform was made to address the logistical challenges that came with working in this environment. Whilst this has inevitably introduced a degree of noise into our dataset, it has also resulted in a larger number of trials than would have otherwise been possible. Our substrate setup means the results are subjectively more applicable to giraffes living in a naturalistic environment, compared with giraffes kept on hard surfaces.

We did not detect significant inter-subject variation in stride length or peak force. Although Giraffe 3 had a history of overgrown forefeet, it does not appear to have affected these gait parameters. Despite this, we observed variation between giraffes in the symmetry of their forelimb GRF_{VERT} profiles (Fig. 5C-D). Varying asymmetry was also evident from an additional (fourth) giraffe from an earlier study, walking at 0.027 to 0.14 Fr. These GRF data (Warner et al., 2013) were gathered under different experimental conditions to the present study, including hard substrate. In light of this, the asymmetrical GRF_{VERT} profile of the forelimb appears to be a consistent feature of giraffe locomotion. We also observed intra-subject variation in the hindlimb GRF_{VERT} profile (Fig. 5E-F). Within the same subject, the profile featured either two or three vertical peaks. The reason for this

variability is unclear. Three-peaked GRF_{VERT} profiles are also seen in elephants (Ren et al., 2010), so this may be a feature of extreme body mass or long limb length.

Linear regression of the Fourier coefficients offers mechanistic insight into how GRF_{VERT} changes over the speed range. Each of the coefficients of the forelimbs increased significantly in magnitude with speed (Fig. 6), resulting in GRF_{VERT} profiles with exaggerated peaks in late stance phase, and lower mid-stance forces. This pattern of change is consistent with findings in walking adults and children, and has been linked to a stiff-limbed pendulum model of walking (Hubel and Usherwood, 2015).

It remains to be seen how much giraffes deviate from dynamic similarity from other mammalian quadrupeds. Dynamic similarity (Alexander and Jayes, 1983) is directly related to geometric similarity, meaning animals which are geometrically similar will move in a dynamically similar fashion (where linear dimensions, time intervals and forces are related by constant factors) at equal dimensionless speed. A giraffe is not geometrically similar to a rhinoceros – giraffes have a metatarsal to femur length ratio of 1.4, compared with 0.33 in *Ceratotherium simum* (Garland and Janis, 1993) – but deviations from dynamic similarity may illustrate how the locomotor system in giraffes has become specialised. Any similarities may give us confidence when extrapolating biomechanical principles from other (cursorial) animals to giraffes, or even from giraffes to their extinct cousins (Basu et al., 2016). For example, giraffes' relative stride length at Fr 0.054 can be predicted using Alexander's power equations (Table II of Alexander and Jayes 1983) with a percentage prediction error (PPE) of 21%; although PPE may be as low as 5% when the full range of dynamic similarity solutions are explored, using the models' confidence intervals. Duty factor yields similar levels of prediction errors (Table 2), and a limb phase of 0.14 is consistent with Fig. 2 of Alexander and Jayes 1983 (when expressed in equivalent terms). A 70:14 gait (Fig. 3) is also found within the continuum of symmetrical gaits of other quadrupedal vertebrates (Hildebrand, 1989). In light of these similarities, we find that giraffes' walking gait is not as functionally distinct as often stated.

We suggest that despite a suite of stark morphological specialisations, giraffes walk using the same mechanistic principles which underlie slow-speed walking in most other mammalian quadrupeds. This does not mean that the gait kinetics or kinematics of giraffes can simply be modelled from other animals. Rather, other models of quadrupedal locomotion can be used to generate testable hypotheses; for example, to test athletic performance at the more extreme ranges of ability in giraffes, or to explain more complex mechanisms (e.g. force, work and power at the level of the limb, joint or musculotendon units) used during walking.

ACKNOWLEDGEMENTS

We thank ZSL Whipsnade Zoo, for allowing us to gather data from their giraffes, and to the staff (and giraffes) for their effort and patience during data collection. Thanks also to the staff and students of the Structure & Motion Laboratory for assisting with experiments; the RVC porters for carrying heavy things; to Luke Grinham for assistance with video analysis; to Jeff Rankin for his assistance in equipment troubleshooting; to Ruby Chang for statistical advice; and to Jim Usherwood and Jorn Cheney for helpful discussions. We acknowledge and thank two anonymous reviewers who improved this paper with their insightful comments.

COMPETING INTERESTS

The authors have no competing interests to declare

AUTHOR CONTRIBUTIONS

All authors designed the experiment, CB and AW installed the experimental setup, CB and JRH carried out data collection. CB prepared the manuscript, with contributions from AW and JRH.

FUNDING

We thank NERC for funding this research (PhD studentship for CB; grant no. NE/K004751/1 to JRH).

DATA AVAILABILITY

Ground reaction force data and associated stride parameters are available to download from Figshare (10.6084/m9.figshare.7297778).

REFERENCES

Alexander, R. and Jayes, A. (1983). A dynamic similarity hypothesis for the gaits of quadrupedal mammals. *Journal of Zoology* **201**, 135-152.

Alexander, R., Maloiy, G., Hunter, B., Jayes, A. and Nturibi, J. (1979). Mechanical stresses in fast locomotion of buffalo (*Syncerus caffer*) and elephant (*Loxodonta africana*). *Journal of Zoology* **189**, 135-144.

Alexander, R. M. and Jayes, A. S. (1980). Fourier analysis of forces exerted in walking and running. *J Biomech* **13**, 383-90.

Alexander, R. M., Langman, V. A. and Jayes, A. S. (1977). Fast locomotion of some African ungulates. *Journal of Zoology* **183**, 291-300.

Basu, C., Falkingham, P. L. and Hutchinson, J. R. (2016). The extinct, giant giraffid Sivatherium giganteum: skeletal reconstruction and body mass estimation. *Biology letters* **12**.

Bates, K. T., Mannion, P. D., Falkingham, P. L., Brusatte, S. L., Hutchinson, J. R., Otero, A., Sellers, W. I., Sullivan, C., Stevens, K. A. and Allen, V. (2016). Temporal and phylogenetic evolution of the sauropod dinosaur body plan. *Royal Society Open Science* **3**.

Benjamini, Y. and Hochberg, Y. (1995). Controlling the false discovery rate: a practical and powerful approach to multiple testing. *Journal of the royal statistical society. Series B (Methodological)*, 289-300.

Bennett, M. B. (2001). Tetrapod Walking and Running. In *eLS*: John Wiley & Sons, Ltd.

Biewener, A. A. (1983). Allometry of quadrupedal locomotion: the scaling of duty factor, bone curvature and limb orientation to body size. *Journal of experimental Biology* **105**, 147-171.

Buchner, H. H. F., Savelberg, H. H. C. M., Schamhardt, H. C. and Barneveld, A. (1997). Inertial properties of Dutch Warmblood horses. *J Biomech* **30**, 653-658.

Cameron, E. Z. and du Toit, J. T. (2007). Winning by a neck: tall giraffes avoid competing with shorter browsers. *The American Naturalist* **169**, 130-135.

Crevier-Denoix, N., Robin, D., Pourcelot, P., Falala, S., Holden, L., Estoup, P., Desquilbet, L., Denoix, J. M. and Chateau, H. (2010). Ground reaction force and kinematic analysis of limb loading on two different beach sand tracks in harness trotters. *Equine veterinary journal* **42**, 544-551.

Dagg, A. and Vos, A. (1968a). Fast gaits of pecoran species. *Journal of Zoology* **155**, 499-506.

Dagg, A. I. (1962). The Role of the Neck in the Movements of the Giraffe. *Journal of Mammalogy* **43**, 88-97.

Dagg, A. I. and Vos, A. d. (1968b). The walking gaits of some species of Pecora. *Journal of Zoology* **155**, 103-110.

Doke, J., Donelan, J. M. and Kuo, A. D. (2005). Mechanics and energetics of swinging the human leg. *Journal of experimental Biology* **208**, 439-445.

Garland, T. and Janis, C. M. (1993). Does metatarsal/femur ratio predict maximal running speed in cursorial mammals? *Journal of Zoology* **229**, 133-151.

Griffin, T. M., Main, R. P. and Farley, C. T. (2004). Biomechanics of quadrupedal walking: how do four-legged animals achieve inverted pendulum-like movements? *Journal of experimental Biology* **207**, 3545-3558.

Hedrick, T. L. (2008). Software techniques for two- and three-dimensional kinematic measurements of biological and biomimetic systems. *Bioinspir Biomim* **3**, 034001.

Hildebrand, M. (1976). Analysis of tetrapod gaits: general considerations and symmetrical gaits. *Neural control of locomotion* **18**, 203-206.

Hildebrand, M. (1989). The quadrupedal gaits of vertebrates. *BioScience* **39**.

Hubel, T. Y. and Usherwood, J. R. (2015). Children and adults minimise activated muscle volume by selecting gait parameters that balance gross mechanical power and work demands. *J Exp Biol* **218**, 2830-9.

Hudson, P. E., Corr, S. A. and Wilson, A. M. (2012). High speed galloping in the cheetah *(Acinonyx jubatus)* and the racing greyhound (*Canis familiaris*): spatio-temporal and kinetic characteristics. *J Exp Biol* **215**, 2425-2434.

Hummel, J. (2006). Giraffe husbandry and feeding practices in Europe. Results of an EEP survey. *6th Congress of the European Association of Zoo and Wildlife Veterinarians, Budapest (Hungary) 24 May 2006 - 28 May 2006*, 71-74.

Innis, A. C. (1958). The behaviour of the giraffe, Giraffa camelopardalis, in the eastern Transvaal. In *Proceedings of the Zoological Society of London*, vol. 131, pp. 245-278: Wiley Online Library.

Kar, D., Issac, K. K. and Jayarajan, K. (2003). Gaits and energetics in terrestrial legged locomotion. *Mechanism and Machine Theory* **38**, 355-366.

Lee, D. V., Bertram, J. E. and Todhunter, R. J. (1999). Acceleration and balance in trotting dogs. *Journal of experimental Biology* **202**, 3565-3573.

Loscher, D. M., Meyer, F., Kracht, K. and Nyakatura, J. A. (2016). Timing of head movements is consistent with energy minimization in walking ungulates. *Proceedings of the Royal Society B: Biological Sciences* **283**.

McMahon, T. A., Valiant, G. and Frederick, E. C. (1987). Groucho running. *Journal of Applied Physiology* **62**, 2326-2337.

Mitchell, G., Roberts, D., van Sittert, S. and Skinner, J. D. (2013). Growth patterns and masses of the heads and necks of male and female giraffes. *Journal of Zoology* **290**, 49-57.

Pandy, M., Kumar, V., Berme, N. and Waldron, K. (1988). The dynamics of quadrupedal locomotion. *Journal of biomechanical engineering* **110**, 230-237.

Parkes, R. S. V. and Witte, T. H. (2015). The foot–surface interaction and its impact on musculoskeletal adaptation and injury risk in the horse. *Equine veterinary journal* **47**, 519-525.

Pfau, T., Hinton, E., Whitehead, C., Wiktorowicz-Conroy, A. and Hutchinson, J. (2011). Temporal gait parameters in the alpaca and the evolution of pacing and trotting locomotion in the Camelidae. *Journal of Zoology* **283**, 193-202.

Pfau, T., Spence, A., Starke, S., Ferrari, M. and Wilson, A. (2009). Modern riding style improves horse racing times. *Science* **325**, 289-289.

Raichlen, D. A., Pontzer, H., Shapiro, L. J. and Sockol, M. D. (2009). Understanding hind limb weight support in chimpanzees with implications for the evolution of primate locomotion. *American Journal of Physical Anthropology* **138**, 395-402.

Ren, L., Miller, C. E., Lair, R. and Hutchinson, J. R. (2010). Integration of biomechanical compliance, leverage, and power in elephant limbs. *Proceedings of the National Academy of Sciences* **107**, 7078-7082.

Shine, C. L., Penberthy, S., Robbins, C. T., Nelson, O. L. and McGowan, C. P. (2015). Grizzly bear (Ursus arctos horribilis) locomotion: gaits and ground reaction forces. *Journal of experimental Biology* **218**, 3102-3109.

Simmons, R. E. and Scheepers, L. (1996). Winning by a neck: sexual selection in the evolution of giraffe. *American Naturalist*, 771-786.

Starke, S. D. and Clayton, H. M. (2015). A universal approach to determine footfall timings from kinematics of a single foot marker in hoofed animals. *PeerJ* **3**, e783.

Warner, S. E., Pickering, P., Panagiotopoulou, O., Pfau, T., Ren, L. and Hutchinson, J. R. (2013). Size-related changes in foot impact mechanics in hoofed mammals. *PLoS One* **8**, e54784.

Witte, T., Knill, K. and Wilson, A. (2004). Determination of peak vertical ground reaction force from duty factor in the horse (*Equus caballus*). *Journal of experimental Biology* **207**, 3639-3648.

Zajac, F. E. (1989). Muscle and tendon: properties, models, scaling, and application to biomechanics and motor control. *Critical reviews in biomedical engineering* **17**, 359-411.

Table 1 Giraffes used in data analysis, with a breakdown of their contributions to the dataset.

Table 2 Stride predictions according to dynamic similarity, and comparisons with giraffe experimental data, including prediction percentage error (PPE). 95% confidence intervals for the predictive exponents are included.

Figure 1 Experimental setup. A wire fence ran parallel to the force plate array, in between the giraffes and equipment. Animal keepers led the giraffes back and forth (left and right) along the force plate array. Sufficient space was allowed for acceleration and deceleration. The remote trigger started 30 seconds of force plate data collection, as well as triggering the LED lights to mark the time on the video recordings. Raw force plate voltages were transduced by the data-acquisition device (DAQ). The GoPro cameras were situated at a perpendicular distance of 5 m from the force plate array.

Figure 2 (A) An adult giraffe showing digital marker system (blue dots) and definition of neck angle (B) Scatter plot of neck range of motion *versus* speed. Linear regressions are shown as a black line in the form $y = au + b$ (see Table S2 for further details). Neck range of motion increased as a function of walking speed ($y = 6.4u + 3.1$, $R^2 = 0.13$, $p = 0.01$), $n = 46$ (C) Time series of the mean neck angle (blue line) and individual trials (grey lines) throughout one forelimb stride, with relative timing of mean forelimb and hindlimb GRFs (red and yellow lines respectively), and contralateral limb GRFs (dashed lines). The neck oscillated twice during each stride, with peak dorsiflexion occurring in the early stance of the left and right forelimb.

Figure 3 Reproduction of Hildebrand's plot for symmetrical gaits of terrestrial vertebrates (Hildebrand, 1976), with overlying giraffe data from the current study. The mean duty factor and limb phase for walking giraffes was 0.7 and 0.14 respectively, and the majority of strides lie within the continuum of previously observed symmetrical gaits. These data show that giraffes use a lateral sequence walk.

Figure 4 (A) Increases in speed were achieved through a marked increase in stride length ($y = 1.2u + 0.8$, $R^2 = 0.54$, $p < 0.01$). (B) Stride duration ($y = -0.75u + 2.9$, $R^2 = 0.55$, $p < 0.01$) fell with speed. Stance duration was longer in the forelimb ($y = -0.87u + 2.4$, $R^2 = 0.6$, $p < 0.01$) than in the hindlimb ($y = -0.55u + 1.9$, $R^2 = 0.62$, $p < 0.01$), resulting in (C) higher duty factor in the forelimb ($y = -0.12u + 0.83$, $R^2 = 0.36$, $p < 0.01$) than the hindlimb ($y = -0.07u + 0.73$, $R^2 = 0.23$, $p < 0.01$).

677

678 Figure 5 (A) Forelimb GRFs were characterised by a double peaked vertical GRF, with the second
679 peak having a greater magnitude, n = 46 (B) Hindlimb GRFs. Shaded areas represent ± 1 standard
680 deviation, n = 29 (C-D) Examples of inter-subject variation in the vertical GRF profiles of the forelimb,
681 and (E-F) intra-subject variation in the vertical GRF of the hindlimb; these profiles were selected to
682 on the basis of their shape, and whether their associated speed was within 1 SD of the mean (to
683 exclude extreme examples).

684 Figure 6 Fourier coefficients changed as a function of speed in the forelimb (A), leading to GRF
685 shapes with exaggerated peaks during late-stance and lower mid-stance forces, but were constant in
686 the hindlimb (B).

687 Figure 7 (A) Peak forces, standardised by body weight (BW) were higher in the fore *versus* hindlimb.
688 In both cases, peak force was consistent across the observed range of speeds. (B) Vertical impulse,
689 standardised by BW and stride duration, did not significantly change with speed in the forelimb ($p = 0.269$) or hindlimb ($p = 0.047$). The ratio of impulses indicated a FL:HL weight distribution of 65:35.

691 Figure 8 Horizontal (A) and vertical (B) tangential accelerations of the neck (red), trunk (blue) and
692 COM (yellow). Neck acceleration was derived from mathematical modelling (Eqns 9, 10, 11) of neck
693 oscillation; COM acceleration was derived from experimentally measured GRFs and limb phase;
694 trunk acceleration was inferred from the subtraction of neck tangential force from COM force.
695 Horizontal trunk and neck acceleration was timed with a phase of 23%, whilst vertical acceleration
696 had a phase of 15%. The phasing of the modelled neck kinematics with COM forces was compared
697 with empirical kinematic data by deriving horizontal (C) and vertical (D) accelerations of the virtual
698 neck (red) and withers (blue) markers, with good agreement between phasing from both
699 methodologies. Thin lines show data from individual trials, thick lines represent mean values.

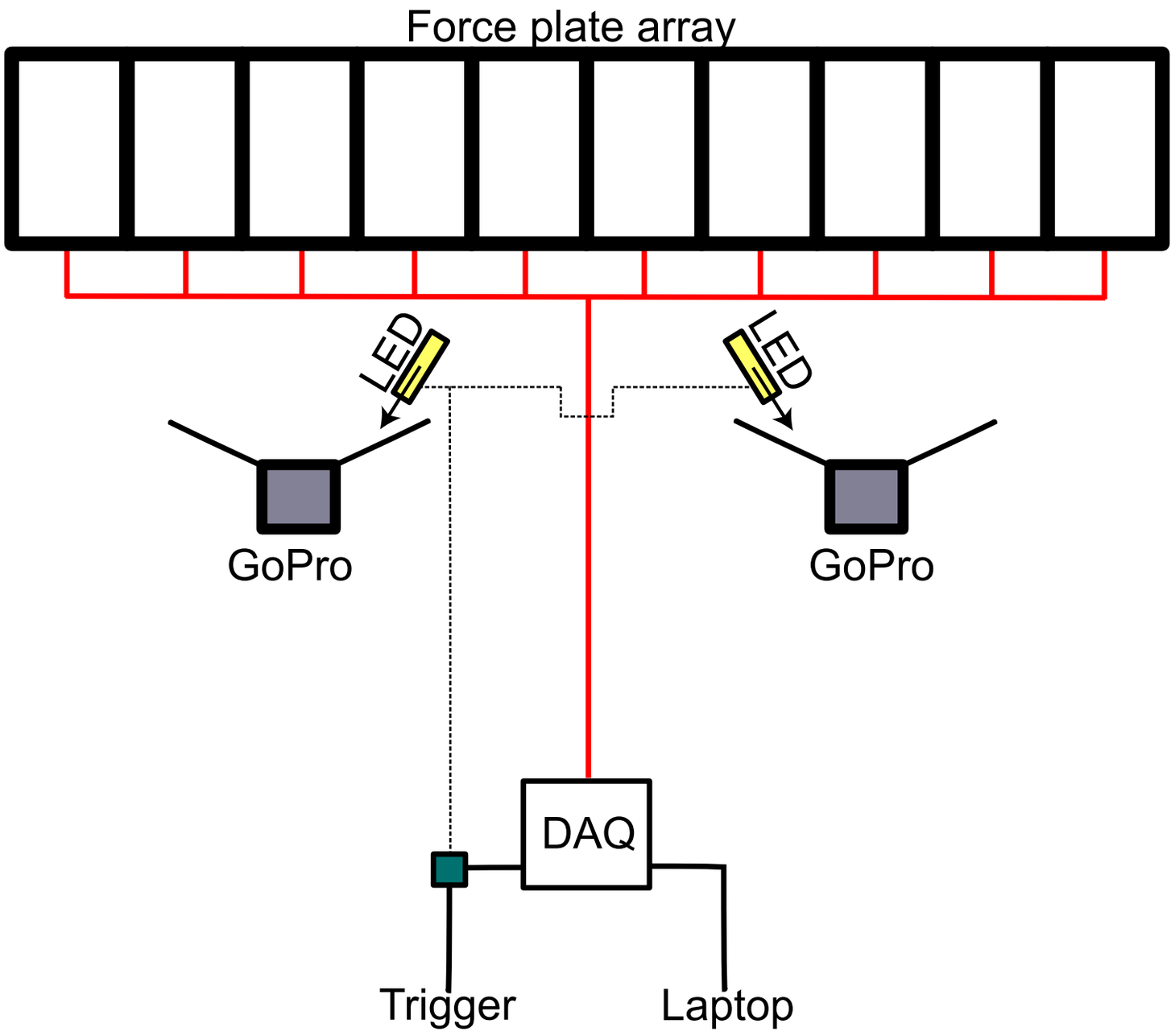
Force plate array
LED
LED
GoPro
GoPro
DAQ
Trigger
Laptop

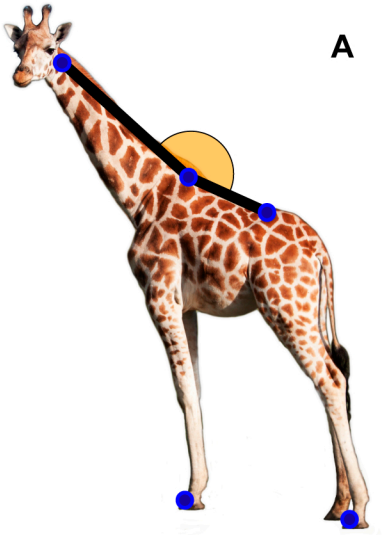

A

B

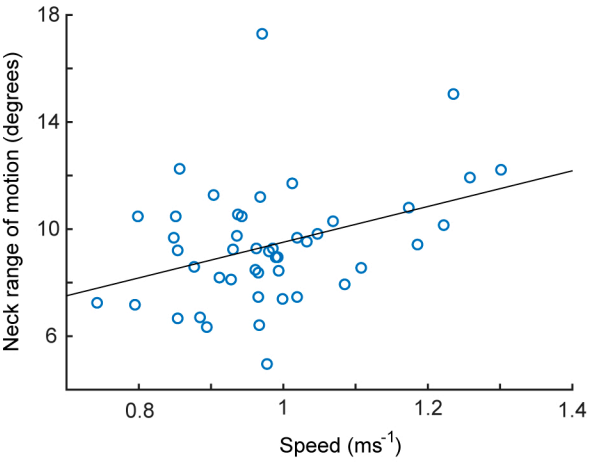
Neck range of motion (degrees)
18
14
10
6
0.8
1
1.2
1.4
Speed (ms-1)

C

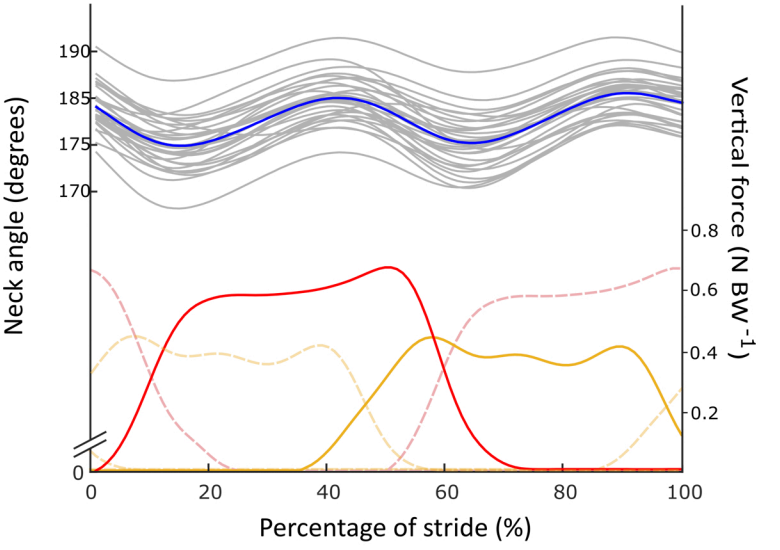
Neck angle (degrees)
190
185
175
170
0
Vertical force (N BW-1)
0.8
0.6
0.4
0.2
0
20
40
60
80
100
Percentage of stride (%)

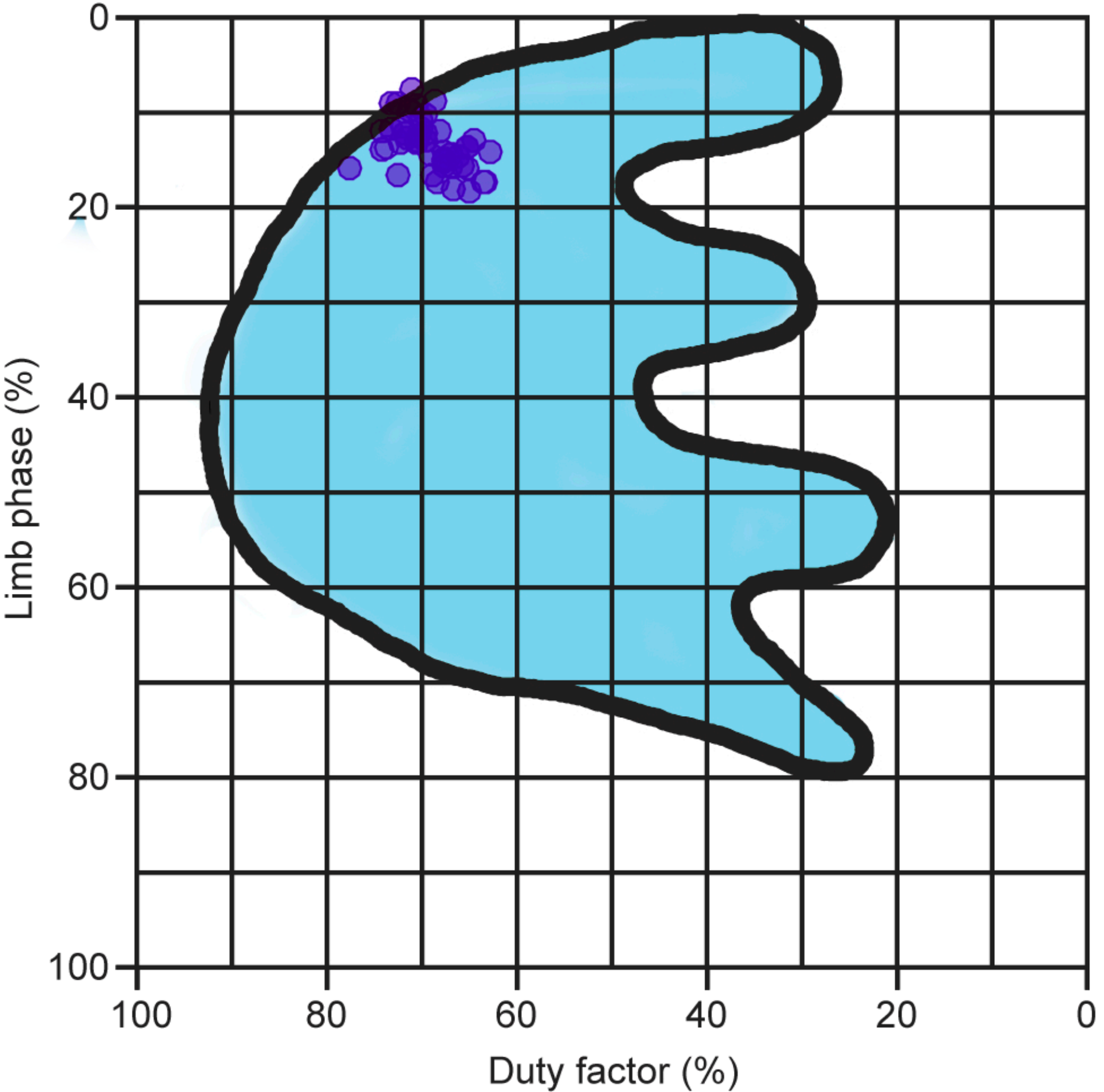
0
20
40
60
80
100
Limb phase (%)
100
80
60
40
20
0
Duty factor (%)

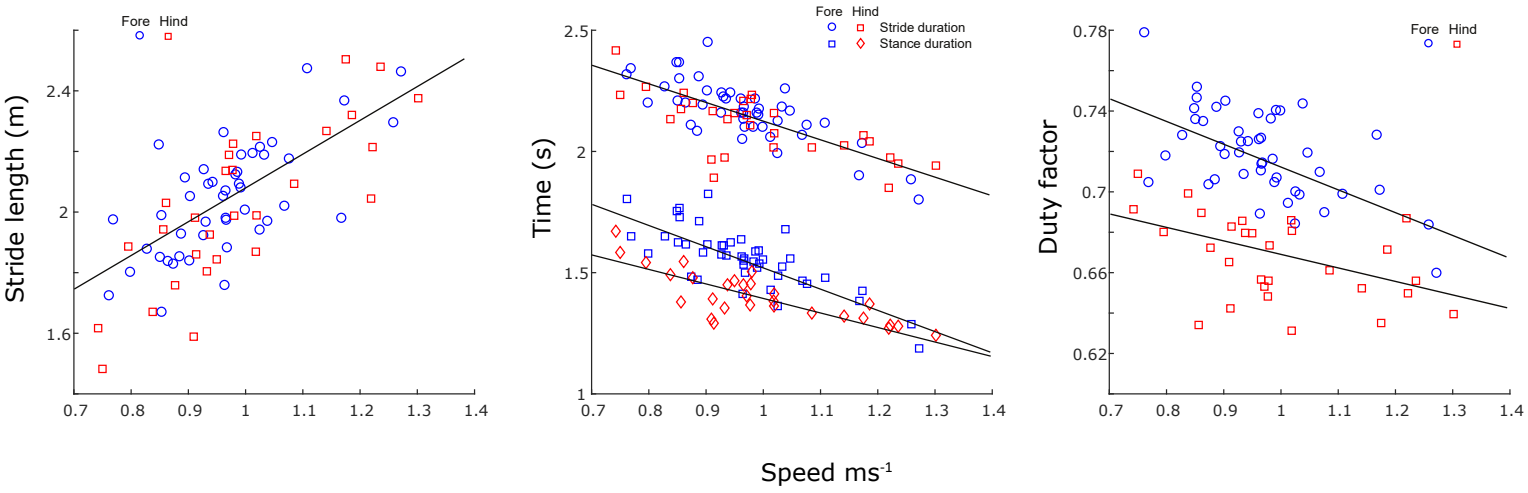
Fore Hind
Stride length (m)
2.4
2
1.6
0.7 0.8 0.9 1 1.1 1.2 1.3 1.4
Fore Hind
Stride duration
Stance duration
Time (s)
2.5
2
1.5
1
0.7 0.8 0.9 1 1.1 1.2 1.3 1.4
Fore Hind
Duty factor
0.78
0.74
0.7
0.66
0.62
0.7 0.8 0.9 1 1.1 1.2 1.3 1.4
Speed ms-1

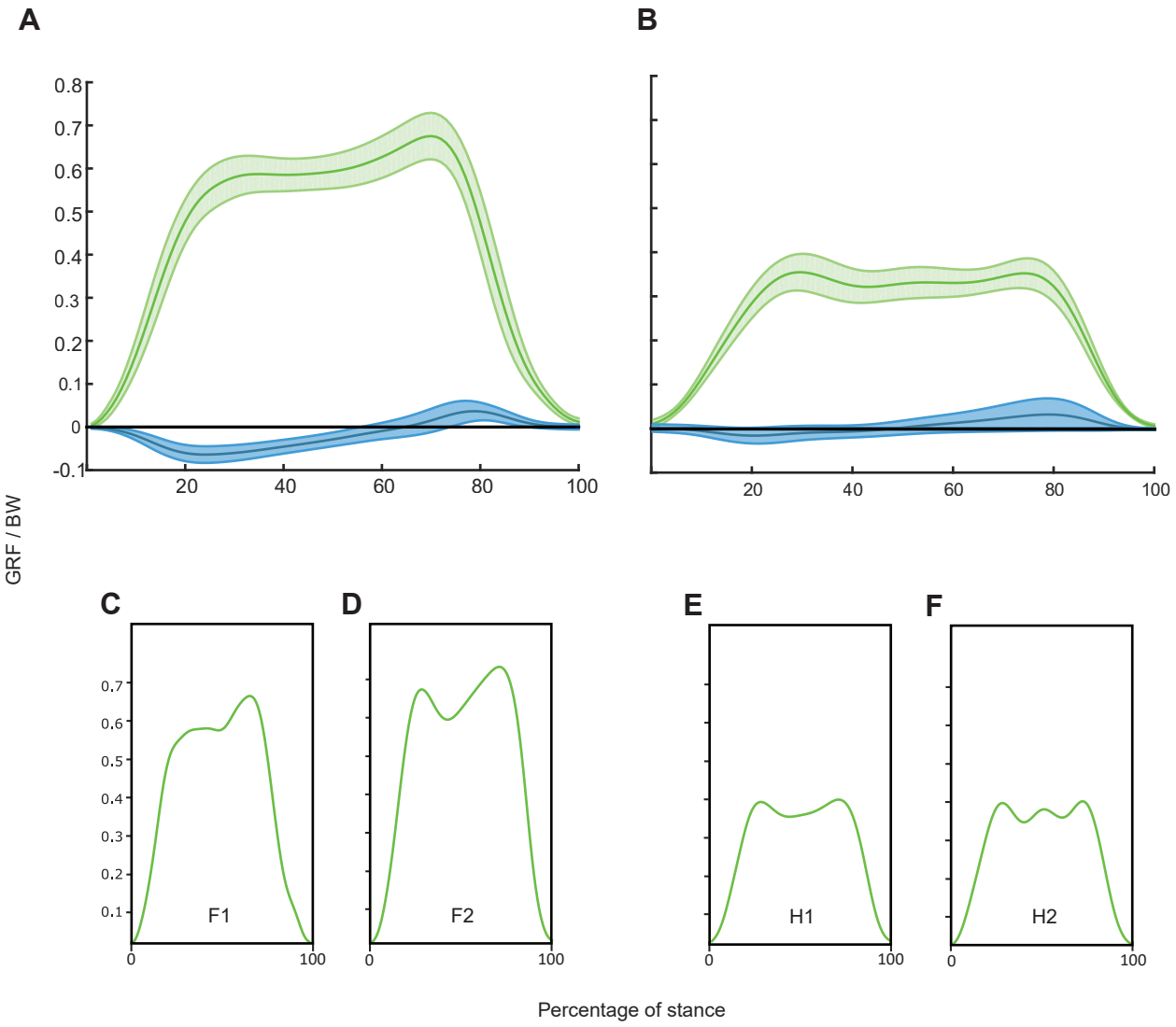
A
B
0.8
0.7
0.6
0.5
0.4
0.3
0.2
0.1
0
-0.1
20
40
60
80
100
GRF / BW
C
D
E
F
F1
F2
H1
H2
0.7
0.6
0.5
0.4
0.3
0.2
0.1
0
100
Percentage of stance

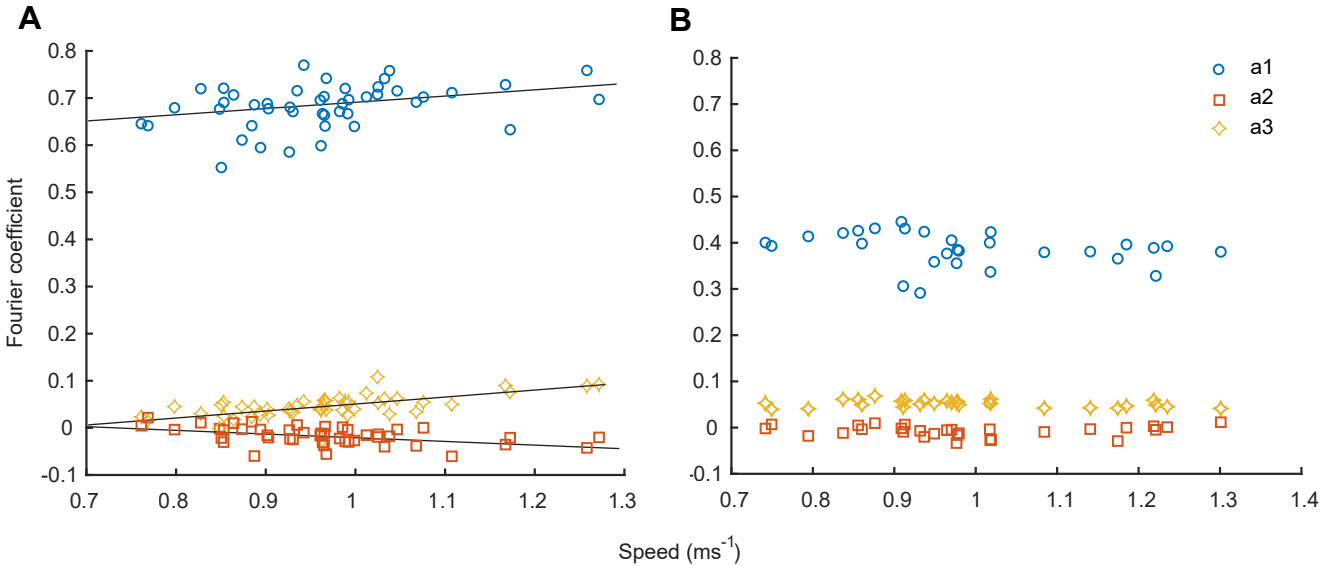
A
B
Fourier coefficient
Speed (ms-1)
a1
a2
a3
0.8
0.7
0.6
0.5
0.4
0.3
0.2
0.1
0
-0.1
0.7
0.8
0.9
1
1.1
1.2
1.3
1.4

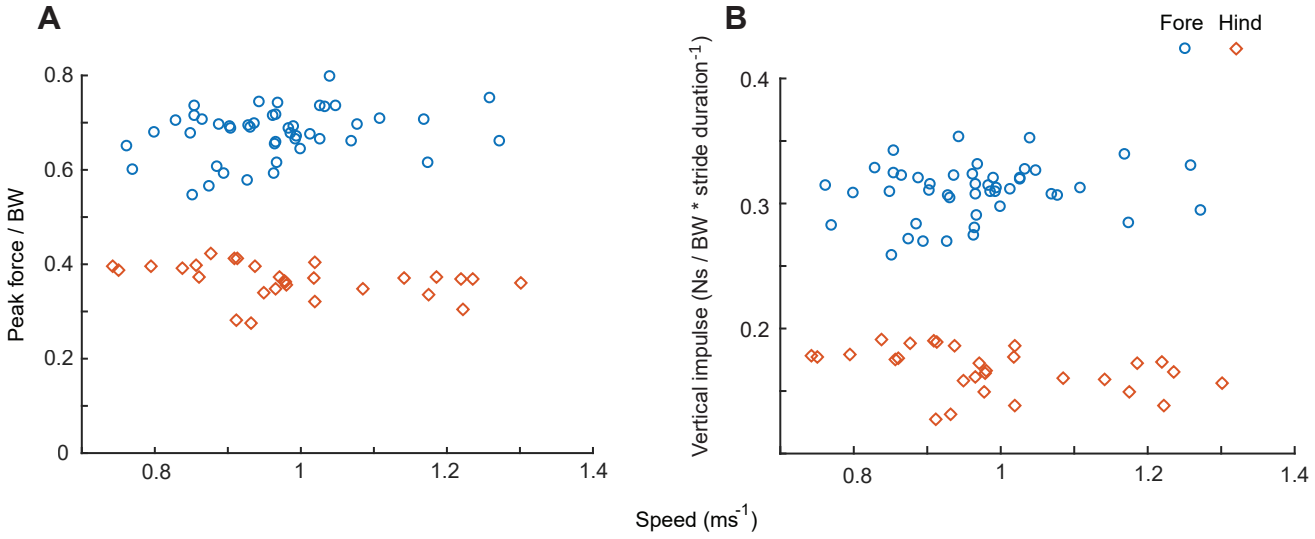
A
B
Fore
Hind
Peak force / BW
Vertical impulse (Ns / BW * stride duration^{-1})
Speed (ms^{-1})
0
0.2
0.4
0.6
0.8
0.2
0.3
0.4
0.8
1
1.2
1.4

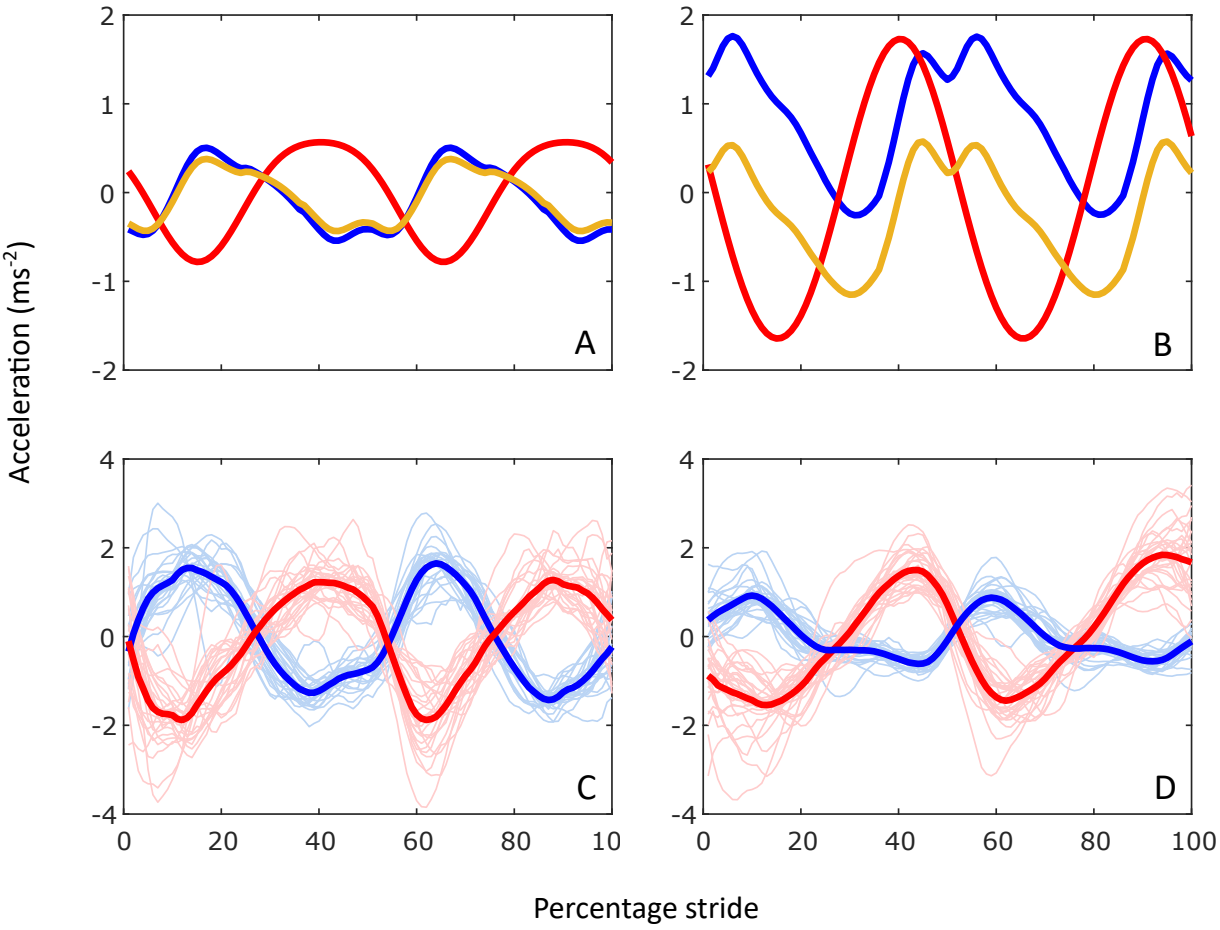
Acceleration (ms-2)
A
B
C
D
Percentage stride

Subject	Sex	Age (years)	Body mass (kg)	Shoulder height (m)	Number trials featuring:		
					Forelimb GRF	Hindlimb GRF	Neck kinematics
1	M	3	800	1.84	4	1	3
2	F	7	750	1.87	8	7	10
3	F	14	780	1.87	34	21	33

Parameter	Equation from Alexander and Jayes 1983	Prediction at mean Fr	Mean experimental value	PPE
Relative stride length (stride length / shoulder height)	$y = 2.4\ (\text{Fr number})^{0.34\ (+-\ 0.1)}$	0.89	1.13	21.3
Fore duty factor	$y = 0.52\ (\text{Fr number})^{-0.14\ (+-\ 0.05)}$	0.78	0.72	-8.7
Hind duty factor	$y = 0.52\ (\text{Fr number})^{-0.18\ (+-0.08)}$	0.88	0.69	-27.4